

NUMERICAL INVESTIGATION ON THE SELF-IGNITION BEHAVIOR OF HIGH PRESSURE HYDROGEN RELEASED FROM THE TUBE

Watanabe H.¹, Matsuo A.²

¹ Graduate School of Science and Technology, Keio University, 3-14-1 Hiyoshi, Kohoku-ku,
Yokohama, Kanagawa, 223-8522, Japan, watanabe0204@keio.jp

² Department of Mechanical Engineering, Keio University, 3-14-1 Hiyoshi, Kohoku-ku,
Yokohama, Kanagawa, 223-8522, Japan, matsuo@mech.keio.ac.jp

ABSTRACT

This paper shows the numerical investigation on the self-ignition behavior of high pressure hydrogen released from the tube. The present study aims to clarify the effect of parameters on the behavior and duration of self-ignition outside the tube using two-dimensional axisymmetric numerical simulation with detailed chemistry. The parameters in this study are release pressure, tube diameter and tube length. The strength of the spherical shock wave to keep chemical reaction and expansion are important factors for self ignited hydrogen jet to be sustained outside the tube. The trend of strength of spherical shock wave is enhanced by higher release pressure and larger tube diameter. The chemical reaction weakens due to expansion and the degree of expansion becomes larger as the spherical shock wave propagates. The characteristic time for the chemical reaction becomes shorter in higher release pressure, larger tube diameter and longer tube diameter cases from the induction time under constant volume assumption. The self ignited hydrogen jet released from the tube is sustained up to the distance where the characteristic time for chemical reaction is shorter than the characteristic time for the flow to expand, and higher release pressure, larger tube diameter and longer tube length expand the distance where the tip flame can propagate downstream. For the seed flame which is the key for jet fire, the larger amount of the ignited volume when the shock wave reaches the tube exit contributes to the formation and stability of the seed flame. The amount of the ignited volume tends to be larger in the longer tube length, higher release pressure and larger tube diameter cases.

1.0 INTRODUCTION

The increase in the population and industrialization keep increasing the energy consumption in the 21st century. At the present moment, the fossil fuel and nuclear power play a major part of energy supply around the world. However, the environmental concern and safety issue pose a problem using conventional energy carrier for the sustainable society. One of the candidates for new energy source is hydrogen. Hydrogen has many merits compared to the conventional energy sources and is expected to be the solution of these problems. Hydrogen does not emit harmful gases such as CO₂ when it burns. In addition, there are many methods to produce hydrogen such as steam reforming and electrolysis of water. Some projects to realize hydrogen economy are underway [1]. In order to introduce hydrogen as the new energy sources, the safety and reliability comparable to fossil fuel must be ensured. However, flammable range of hydrogen-air mixture is much wider than that of conventional fuel such as CH₄ and C₃H₈ and minimum ignition energy is order of 10⁻² mJ, which is much smaller than conventional fuel and can be ignited by static electricity. Also, high pressure storage is needed to compensate the low energy density per unit mass. If hydrogen should leak from high pressure storage tank or pipe, self-ignition occurs even in the absent of ignition source and transits to a jet fire which may cause severe damage to the human and properties.

Many experimental and numerical research have been conducted to understand the hydrogen self-ignition and jet fire caused by high pressure hydrogen release [2-10]. Hydrogen self-ignition and transition to jet fire are affected by release pressure, rupture time, tube diameter, tube length and obstacle shape inside the tube. Mogi *et al.* [2] investigated the effect of tube length, tube diameter on the hydrogen self-ignition and confirmed that smaller tube diameter and longer tube length increase the possibility of self-ignition. They reported that when a hydrogen jet fire is produced by self-ignition, the flame is held at the pipe outlet and self-ignition is initiated at the outer edge of the jet. From the numerical analysis, J. X. Wen *et al.* [6] comprehensively investigated the effect of rupture time, release pressure, tube length and tube diameter on the likelihood of self-ignition.

Based on their simulation results, significant amount of shock-heated air and well developed partially premixed flames make the flame maintain after the spouting from the tube. Also, they suggested that the initial flame transits to jet fire by the seed flame stabilizing around the tube. From the previous researches mentioned above, the factor to affect the self-ignition of hydrogen inside the tube and the transition to jet fire have already clarified. However, the effective parameter on the self-ignition behavior of hydrogen outside the tube and the distance where the tip flame is extinguished have not revealed yet. Therefore, this study aims to clarify the effect of parameters on the behavior and duration of the self-ignition of high pressure hydrogen released from the tube using two-dimensional axisymmetric numerical simulation with detailed chemistry.

2.0 NUMERICAL DETAILS

2.1 Numerical Method

The governing equations are two-dimensional compressible Navier-Stokes equation and conservation equation of chemical species. Ideal gas equation of state is employed.

$$\frac{\partial \hat{\mathbf{Q}}}{\partial t} + \frac{\partial (\hat{\mathbf{E}} - \hat{\mathbf{E}}_v)}{\partial \xi} + \frac{\partial (\hat{\mathbf{F}} - \hat{\mathbf{F}}_v)}{\partial \eta} + (\hat{\mathbf{H}} - \hat{\mathbf{H}}_v) = \hat{\mathbf{S}} \quad (1)$$

$$\hat{\mathbf{Q}} = \frac{1}{J} \begin{bmatrix} \rho \\ \rho u \\ \rho v \\ e \\ \rho_i \end{bmatrix}, \quad \hat{\mathbf{E}} = \frac{1}{J} \begin{bmatrix} \rho U \\ \rho u U + \xi_x p \\ \rho v U + \xi_y p \\ (e + p)U \\ \rho_i U \end{bmatrix}, \quad \hat{\mathbf{F}} = \frac{1}{J} \begin{bmatrix} \rho V \\ \rho u V + \eta_x p \\ \rho v V + \eta_y p \\ (e + p)V \\ \rho_i V \end{bmatrix}, \quad \hat{\mathbf{E}}_v = \frac{1}{J} \begin{bmatrix} 0 \\ \xi_x \tau_{xx} + \xi_y \tau_{xy} \\ \xi_x \tau_{yx} + \xi_y \tau_{yy} \\ \xi_x \beta_x + \xi_y \beta_y \\ \xi_x \rho D_i \frac{\partial Y_i}{\partial x} + \xi_y \rho D_i \frac{\partial Y_i}{\partial y} \end{bmatrix},$$

$$\hat{\mathbf{F}}_v = \frac{1}{J} \begin{bmatrix} 0 \\ \eta_x \tau_{xx} + \eta_y \tau_{xy} \\ \eta_x \tau_{yx} + \eta_y \tau_{yy} \\ \eta_x \beta_x + \eta_y \beta_y \\ \eta_x \rho D_i \frac{\partial Y_i}{\partial x} + \eta_y \rho D_i \frac{\partial Y_i}{\partial y} \end{bmatrix}, \quad \hat{\mathbf{H}} = \frac{1}{y} \frac{1}{J} \begin{bmatrix} \rho v \\ \rho u v \\ \rho v^2 \\ (e + p)v \\ \rho_i v \end{bmatrix}, \quad \hat{\mathbf{H}}_v = \frac{1}{y} \frac{1}{J} \begin{bmatrix} 0 \\ \tau_{xy} \\ 2\mu \left(\frac{\partial v}{\partial y} - \frac{v}{y} \right) \\ \tau_{yx} u + \tau_{yy} v + \kappa T_y \\ \eta_x \rho D_i \frac{\partial Y_i}{\partial x} + \eta_y \rho D_i \frac{\partial Y_i}{\partial y} \end{bmatrix}, \quad \hat{\mathbf{S}} = \frac{1}{J} \begin{bmatrix} 0 \\ 0 \\ 0 \\ 0 \\ \omega_i \end{bmatrix}$$

$$\rho = \sum_{i=1}^n \rho_i, \quad Y_i = \rho_i / \rho, \quad U = \xi_x u + \xi_y v, \quad V = \eta_x u + \eta_y v, \quad \beta_x = u \tau_{xx} + v \tau_{xy} - q_x, \quad \beta_y = u \tau_{yx} + v \tau_{yy} - q_y, \quad J = 1 / (x_{\xi} y_{\eta} - x_{\eta} y_{\xi}) \quad (2)$$

$$p = \sum_{i=1}^{Ns} \rho_i R_i T \quad (3)$$

$$e = \sum_{i=1}^{Ns} \rho_i h_i - p + \frac{\rho}{2} (u^2 + v^2) \quad (4)$$

where ρ – density; u - x direction velocity; v - y direction velocity; p – pressure; e - total energy; T – temperature; J – Jacobian; τ - shear stress; q - heat flux; μ – viscosity; κ - thermal conductivity; D - diffusion coefficient; Y - mass fraction; ω - reaction rate; h – enthalpy; R - gas constant; Ns - the number of chemical species; subscript i means the species i .

The Yee's non MUSCL type 2nd order TVD upwind scheme [12] is used for discretization of convective term, and diffusion term is discretized by 2nd order accurate central differential scheme. The hydrogen-oxygen chemical reaction is modeled by detailed chemical kinetics proposed by Hong *et al.* [13], which considers 9 species (H_2 , O_2 , H_2O , H , O , OH , HO_2 , H_2O_2 , N_2) and 20 elemental

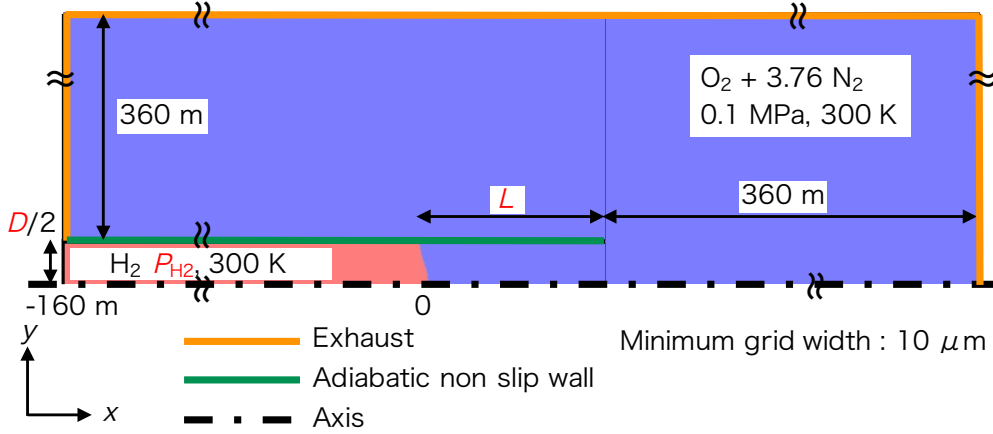


Figure 1. Computational target and initial condition

reactions. The time integration for the chemical source term is conducted by robust MTS method [14] to avoid stiffness and integrate source term efficiently. NASA thermochemical polynomials [15] are used in order to calculate the value of species thermochemical properties. As for the transport properties, gas viscosity and thermal conductivity but for HO_2 are estimated using the method by Gordon *et al.* [16]. For HO_2 mixture, viscosity and thermal conductivity are calculated by Chapman-Enskog method and Eucken method, respectively. Diffusion coefficient for pure species is evaluated by Chapman-Enskog method. Wilke method and Wassiljewa method are used for the estimating multicomponent gas viscosity and thermal conductivity based on the pure species value.

2.2 Computational target and initial condition

Figure 1 shows the computational target and initial condition. The computational target is inside and outside the tube from high pressure hydrogen tank. The computational domain is set large enough for compression and expansion wave not to reach the boundary during the simulation. The tube length from the initial diaphragm position is L and tube diameter is D . Initial pressure, temperature and composition of ambient region are 0.1 MPa, 300 K and $\text{O}_2 + 3.76 \text{ N}_2$, respectively. High pressure hydrogen whose pressure and temperature are P_{H_2} and 300 K is set inside the tube. According to the previous research [8,9], the initial diaphragm shape affects the behavior of self-ignition and initial diaphragm is modeled as the equation (4) referring ref. [9].

$$x_c = 0.05D \cos\left(\pi \frac{2y}{D}\right) \quad (5)$$

where x_c - the diaphragm shape position. Minimum grid width is $10 \mu\text{m}$ to capture self-ignition and maximum grid point is 12726×2801 . The parameters utilized in this study are tube length L , tube diameter D and release pressure P_{H_2} and their values are $D = 3, 6, 10 \text{ mm}$, $L = 0, 30, 45, 60, 90 \text{ mm}$ and $P_{\text{H}_2} = 6.5, 10.0, 14.5, 20.0 \text{ MPa}$. The boundary condition of solid tube wall is adiabatic non slip wall condition and axis condition is applied to the axis line. The other boundary is exhaust condition.

2.3 Validation of present numerical model

Validation of present numerical model is confirmed through the shock propagation speed and induction time for hydrogen-air mixture. Figure 2 shows the relationship between the shock propagation speed inside the tube and hydrogen release pressure. The theoretical shock propagation speed is derived from the Rankin-Hugoniot equation. The calculation condition is as follows. The tube diameter D is 10 mm and release pressure P_{H_2} is 6.5, 10.0, 14.6, 20.0 MPa. Experimental data by Mogi *et al.* [2] which are obtained using the same diameter tube (10 mm) are also plotted in the Fig. 2. From the comparison among the theoretical, experimental and present simulation results, present simulation results show good agreement with both theoretical and experimental data. To show the validity of the chemical reaction, the induction time of hydrogen-air mixture is compared with experimental data

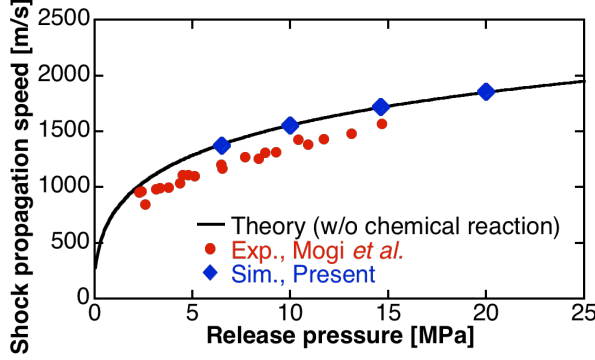


Figure 2. Shock propagation speed

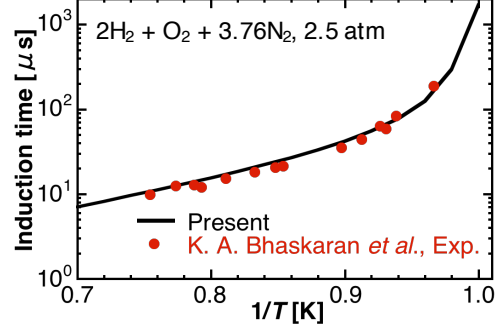


Figure 3. Induction time

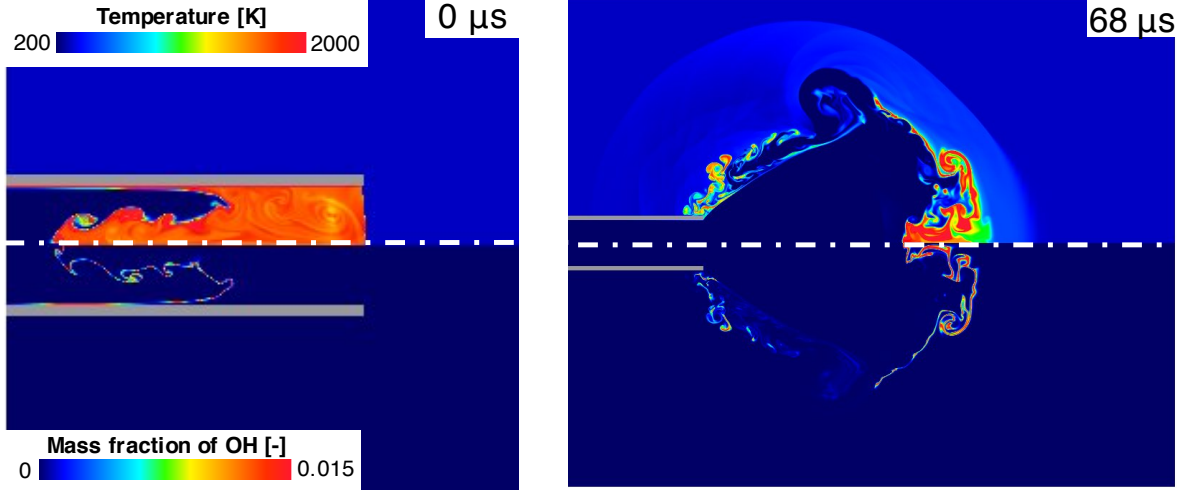


Figure 4. Temperature and mass fraction of OH distribution
($D = 10$ mm, $L = 90$ mm, $P_{H_2} = 20.0$ MPa)

conducted by K. A. Bhaskaran *et al.* [16]. Target mixture is stoichiometric hydrogen-air mixture whose initial pressure is 2.5 atm. Figure 3 shows the relationship between the induction time and reverse of the temperature. Present results using reaction model by Hong *et al.* [12] show good agreements with experimental results in Fig. 3. From Figs. 2 and 3, the present numerical model can capture the compressible flow and reproduce the chemical reaction.

3.0 RESULTS AND DISCUSSION

3.1 Flowfield of self-ignition of high pressure hydrogen released from the tube

The flowfield of the self-ignition of high pressure hydrogen released from the tube are shown in this section. The calculation conditions are $D = 10$ mm, $L = 90$ mm and $P_{H_2} = 20.0$ MPa. Normalized equivalence ratio [18] is introduced to estimate the mixing. Normalized equivalence ratio is defined as the following equation.

$$\phi' = \frac{\phi}{1 + \phi} \quad (6)$$

Where, ϕ – equivalence ratio. Normalized equivalence ratio becomes 0.5 for the stoichiometric mixtures. The time when the shock wave reaches tube exit is set as 0 s in this study. Figure 4 shows the temperature and mass fraction of OH distribution at 0 μ s and 68 μ s after hydrogen reaches the tube exit and Fig. 5 shows the x direction velocity and normalized equivalence ratio distribution at 20 μ s and 68 μ s. Before hydrogen leaks from the tube, self ignition occurs inside the tube from the boundary layer owing to the Kelvin-Helmholtz instability and near the center axis due to the Rayleigh-Taylor instability as previous researches [6-10] in Fig. 4 at 0 μ s for the calculation condition. After spouting

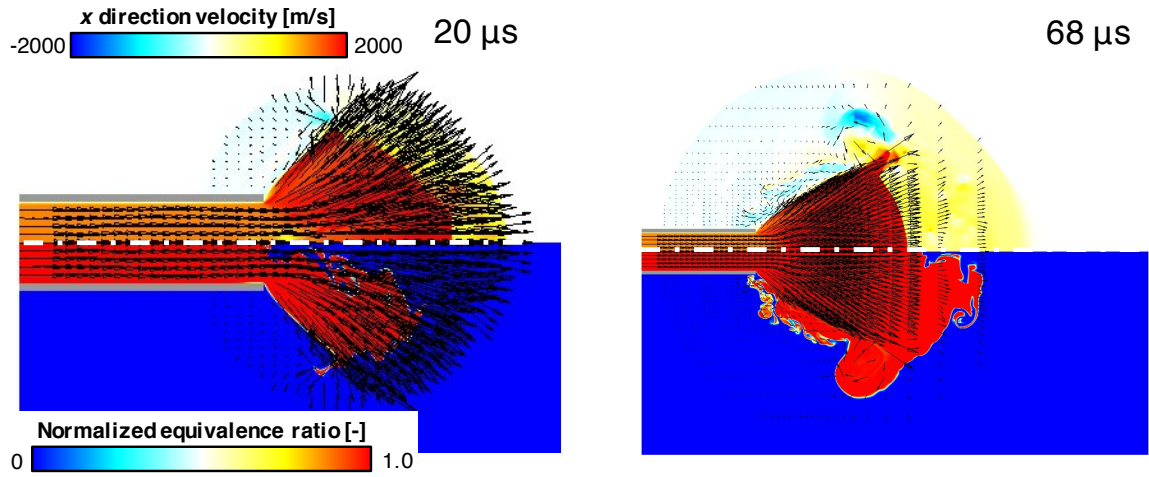


Figure 5. x direction velocity and normalized equivalence ratio distribution
($D = 10$ mm, $L = 90$ mm, $P_{H_2} = 20.0$ MPa)

from the tube, hydrogen jet underexpands and spherical shock wave propagates outside the tube. Spherical shock compresses the ambient air and increases the temperature, which sustains the chemical reaction at the contact surface and makes the flame propagate downstream as shown in Fig. 4 at $68 \mu s$. Velocity shear layer appears from the edge of the tube due to the velocity difference between the underexpanded jet and ambient air compressed by spherical shock. Vortex is generated from the tube edge by this velocity shear layer in Fig. 5 and encompasses the shock heated and ignited mixtures. Encompassed ignited mixtures move to the tube edge by the reverse flow as shown in velocity distribution in Fig. 5. In addition, the recirculation region at the tube edge promotes mixing from Fig. 5 and sustains reaction, which forms and stabilizes the seed flame. Although the spherical shock wave weakens and chemical reaction tends to be quenched due to the expansion as the time passes, the flame still exists up to the calculation time.

3.2 The effect of parameters on the self-ignition of hydrogen released from the tube

The effect of parameters on the behavior and duration of the self-ignition of hydrogen released from the tube is shown in this section. First of all, the parameter study on the tube length is carried out. The calculation conditions are $D = 10$ mm, $L = 45$ mm and $P_{H_2} = 20.0$ MPa, which is the half of the tube length presented in the previous section and other conditions are same. Figure 6 shows the temperature and mass fraction of OH distribution at $0 \mu s$ and $68 \mu s$ from the leakage in the case of $D = 10$ mm, $L = 45$ mm and $P_{H_2} = 20.0$ MPa, respectively. By shortening the tube length, the time that can be spent on chemical reaction and the mixing becomes short. As the result, the shock heated and ignited volume decrease and less mixed mixtures are formed before the leakage compared to the longer tube length case from the comparison of Figs. 4 and 6 at $0 \mu s$. The encompassed ignited volume by the vortex from the edge of the tube becomes smaller, and smaller seed flame is generated in shorter tube case. At the $68 \mu s$ after the leakage from the tube, OH mass fraction shows the smaller value and temperature is lower in Figs 4 and 6, meaning that the flame front is much weakened. The less ignited volume and insufficient mixing before leakage make it difficult to endure the underexpansion and compensate the heat loss due to the expansion. Figure 7 shows over 2000 K volume outside tube history and production rate for OH history to indicate the effect of the tube length on the reactivity of hydrogen jet qualitatively. The temperature does not becomes over 2000 K without chemical reaction in the present condition and the region over 2000 K is regarded as the flame. From Fig. 7(a), the over 2000 K volume outside the tube increases as time passes and flame expands, and the increase rate of over 2000 K volume is higher in longer tube length case despite the same release pressure and tube diameter. In addition, the production for OH is more active and shows higher value in longer tube length case. Longer tube length enhances the reactivity of hydrogen due to longer time for mixing and reaction to occur inside the tube, which enlarges the distance where the tip flame can propagate downstream and helps the formation of larger seed flame near the tube edge.

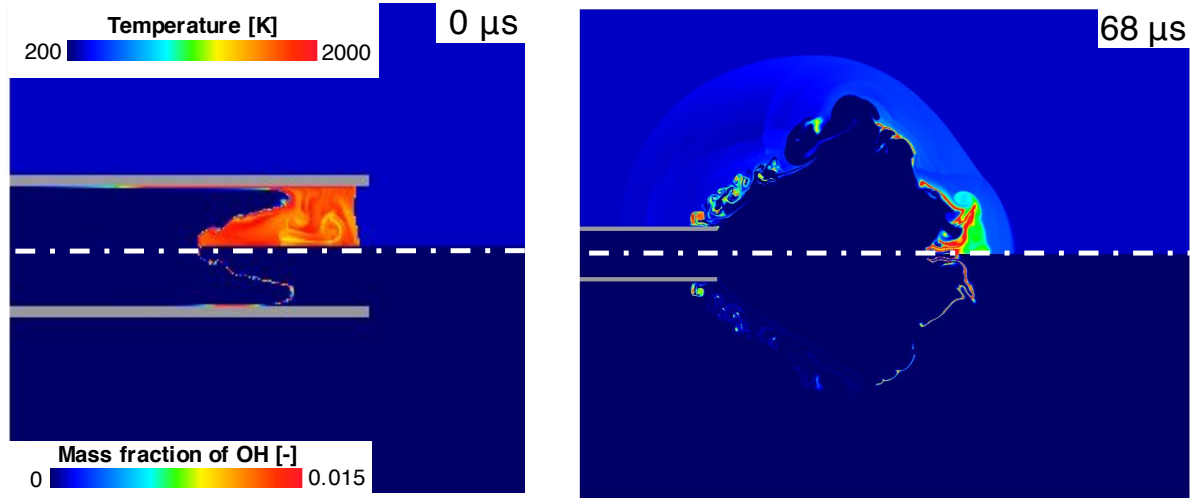
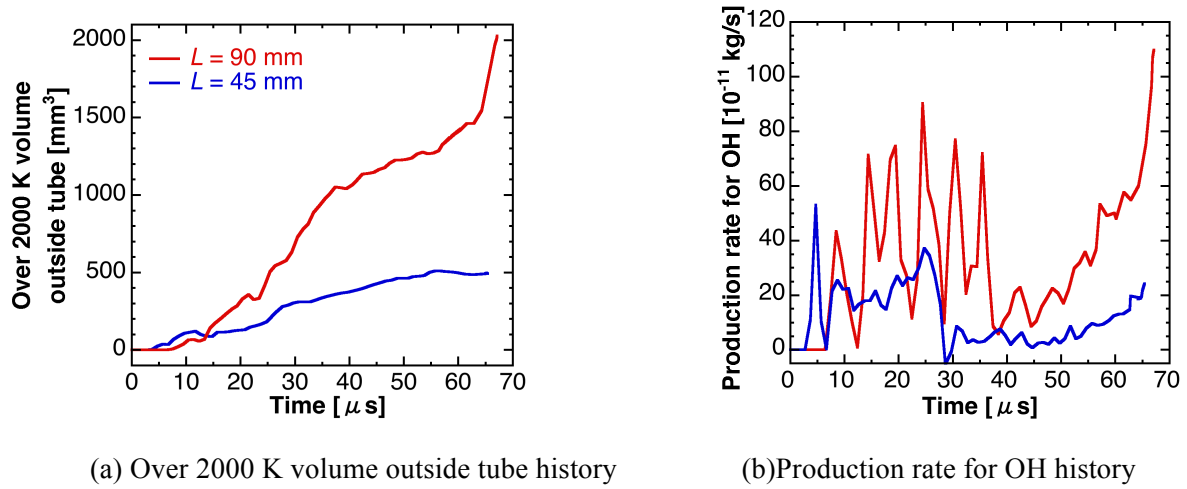


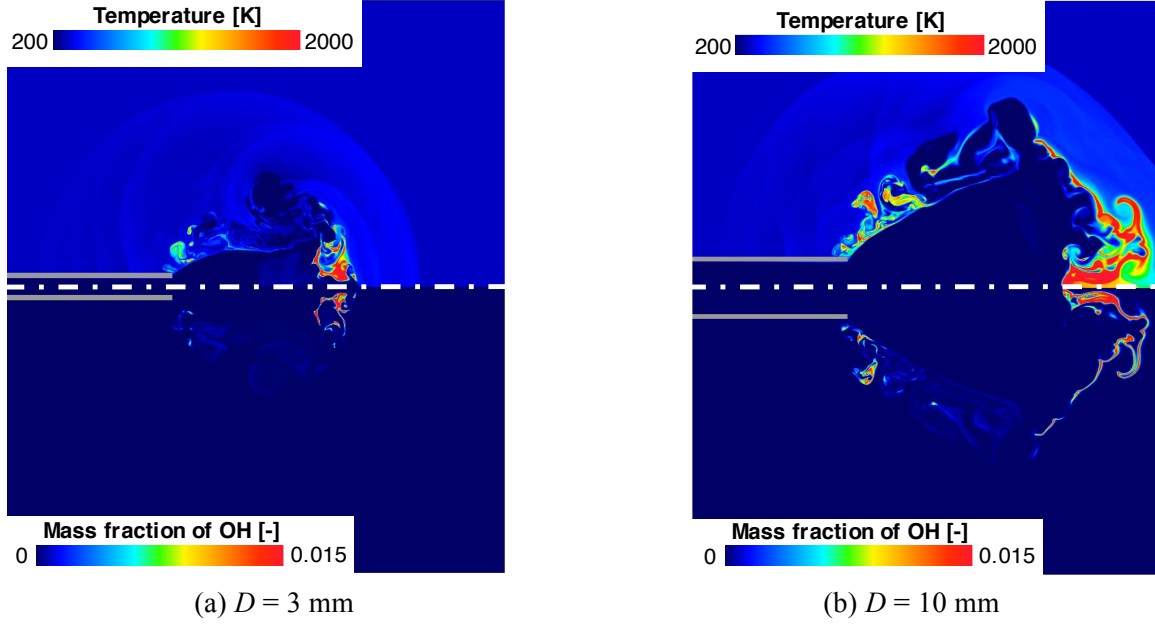
Figure 6. Temperature and mass fraction of OH distribution
($D = 10$ mm, $L = 45$ mm, $P_{H_2} = 20.0$ MPa)



(a) Over 2000 K volume outside tube history (b) Production rate for OH history
Figure 7. The effect of tube length on the reactivity of hydrogen jet ($D = 10$ mm, $P_{H_2} = 20.0$ MPa)

Next, the effect of tube diameter on the self-ignition of hydrogen released from the tube is focused on. The calculation conditions for the tube diameter effect are $L = 90$ mm, $P_{H_2} = 14.5$ MPa and $D = 3, 10$ mm. Figure 8 shows temperature and mass fraction of OH distribution at $68 \mu s$ after the leakage from the tube in the case of $D = 3, 10$ mm with $L = 90$ mm, $P_{H_2} = 14.5$ MPa. The behavior of the flame is different by changing tube diameter even in the same release pressure and tube length. The tip flame is much larger and it propagates downstream further in the larger tube diameter case. Reaction front exists not only around the center axis but also near the tube edge as the seed flame compared to the smaller tube diameter case from the mass fraction of OH distribution in Fig. 8. Figure 9 shows time deviation of over 2000 K volume outside tube history and production rate for OH history to indicate the effect of the tube diameter on the reactivity of hydrogen jet qualitatively. Larger tube diameter case under the same release pressure and tube length shows higher value of time deviation of over 2000 K volume outside tube and production rate for OH. From Fig. 9, it can be confirmed that reactivity and duration of the self-ignited hydrogen jet are enhanced by larger tube diameter.

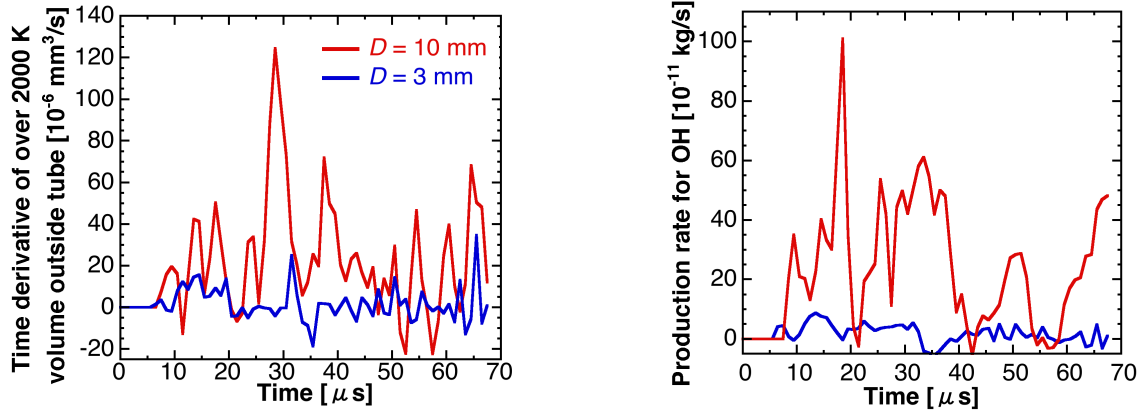
The tube length and tube diameter affect the behavior and duration of the self-ignite hydrogen outside the tube. The mechanism for the self-ignited jet to be sustained outside the tube is as follows. The shock wave released from the tube compresses the ambient air and air mixes with hydrogen at the contact surface, which sustains the chemical reaction. The strength of the spherical shock wave and whether the sufficient mixing is achieved or not are important factors for the self-ignition to be sustained. At the same time, the hydrogen jet expands and temperature and pressure decreases as the



(a) $D = 3$ mm

(b) $D = 10$ mm

Figure 8. Temperature and mass fraction of OH distribution at $68 \mu\text{s}$ after the leakage from the tube ($L = 90$ mm, $P_{\text{H}_2} = 14.5$ MPa)



(a) Time deviation of over 2000 K volume outside tube history

(b) Production rate for OH history

Figure 9. The effect of tube diameter on the reactivity of hydrogen jet ($L = 90$ mm, $P_{\text{H}_2} = 14.5$ MPa)

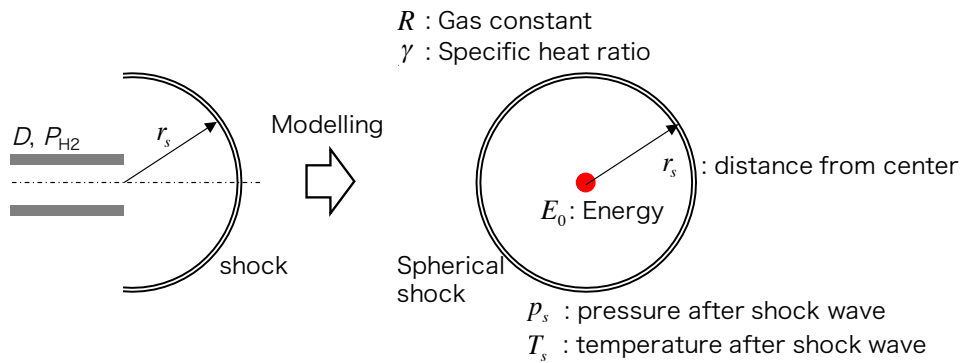


Figure 10. Schematic of modelling of spherical shock wave from the tube as the spherical shock wave from point source

hydrogen jet leaks from the tube, which makes the self ignited hydrogen jet to be extinguished. Therefore, the self ignited hydrogen jet from the tube is sustained and propagates downstream as long as the chemical reaction occurs before the flame extinguishes due to expansion. In order to consider the distance where the self ignited hydrogen can propagate with keeping reaction, the trend of strength of the spherical shock wave is estimated by modelling the high pressure hydrogen release from the

tube as the spherical shock wave propagation using Point Blast Theory [19]. The schematic of modelling of spherical shock wave from the tube as the spherical shock wave from point source is shown in Fig. 10. Although the phenomena of high pressure hydrogen release and spherical shock wave propagation from point source are different, the trend of strength of the spherical shock can be roughly understood. Under the assumption that the initial gas density is constant and the spherical shock wave, the value of pressure and temperature directly behind the shock wave front are obtained from the below equations.

$$p_s = \frac{2E_0}{\alpha} \delta^2 \frac{r_s^{-3}}{\gamma+1} \quad (7)$$

$$T_s = \frac{2(\gamma-1)}{R(\gamma+1)^2} \delta^2 \frac{E_0}{\alpha \rho_0} r_s^{-3} \quad (8)$$

$$\delta = \frac{2}{5} \quad (9)$$

where, p_s – pressure behind the shock wave front ; T_s – temperature behind the shock wave front ; E_0 – total energy of the source ; r_s – distance from the center ; ρ_0 – initial gas density ; R - gas constant, γ – specific heat ratio ; α – constant parameter depending on specific heat ratio.

The schematic of pressure and temperature after the shock wave as the function of distance from the center is shown in Fig. 11. Clearly, the pressure and temperature after the spherical shock wave decrease as it propagates due to expansion. The strength of the spherical shock depends on the total energy of the source from the equation (7)(8). The total energy of the source increases in higher release pressure and larger tube diameter cases for the hydrogen jet. The value of the pressure and temperature behind the spherical shock wave increases and keeps higher in larger total energy of source cases as shown in Fig. 11. Also, the flame is extinguished if the pressure and temperature after shock wave becomes low to sustain chemical reaction. The chemical reaction weakens due to expansion and the degree of expansion becomes larger as the spherical shock wave propagates.

In order to indicate the relationship between the strength of the shock wave and self-ignition, pressure after the shock wave and the induction time under the condition that the initial temperature and pressure are the value after the shock wave and composition is stoichiometric hydrogen-air from zero dimensional constant volume calculation are plotted in the Fig. 12. Induction time is shorter in the higher pressure after the shock wave case because temperature after the shock wave increases. Therefore, the larger tube diameter and higher release pressure lead to the higher pressure after the shock wave, resulting in the shorter induction time. The longer tube length tends to increase the ignited volume and makes it easier for self-ignition to occur by mixing and heat conduction from the ignited mixtures to unburned mixture. The induction time under the condition that the initial pressure is after shock wave value and initial temperature is the temperature plus 100 K after the shock wave in stoichiometric hydrogen-air mixture are also shown in Fig. 12. Increasing initial temperature by heat conduction from larger ignited mixture due to longer tube length makes induction time short compared to that with temperature after the shock wave.

The flame front propagating downstream can be sustained if the chemical reaction occurs and sustains the self ignited hydrogen jet before the flame is extinguished due to expansion. That is, the characteristic time t_{chem} for chemical reaction, i.e. induction time, is shorter than the time required for the state to be lower than the condition for the flame to be extinguished $t_{\text{expansion}}$. Figure 13 shows the schematic of the flame holding distance. The distance where the tip flame can propagate downstream is gray area in Fig. 13. Larger tube diameter, higher release pressure and longer tube length make induction time short, which expands area where the tip flame can propagate downstream. To confirm this concept, x - t diagrams of pressure on the axis line outside the tube for $D = 3, 10$ mm in the case of $L = 90$ mm, $P_{\text{H}_2} = 14.5$ MPa are shown in Fig. 14. The values after the shock wave keep higher in the larger tube diameter case from the Point Blast Theory in Figs. 11 and 14, and the tip flame survives further downstream from Fig. 8. In conclusion, the duration of the self-ignition outside the tube

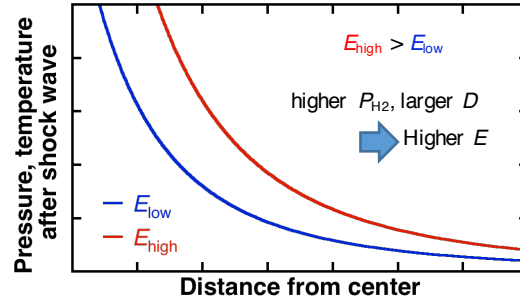


Figure 11. Schematic of pressure and temperature after the shock wave as the function of distance from center

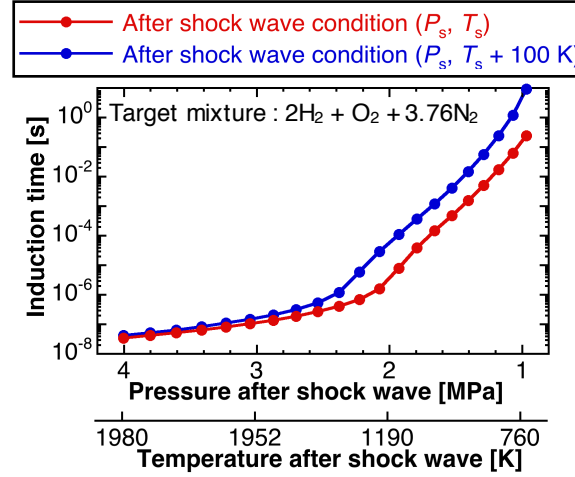


Figure 12. Pressure after shock wave and induction time (target mixture : $2\text{H}_2 + \text{O}_2 + 3.76 \text{N}_2$)

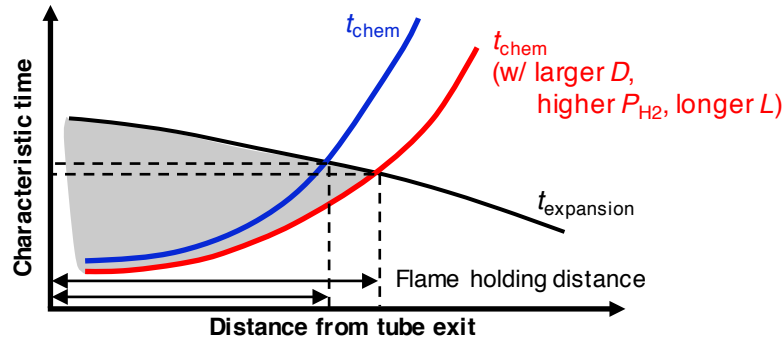


Figure 13. Schematic of the flame holding distance

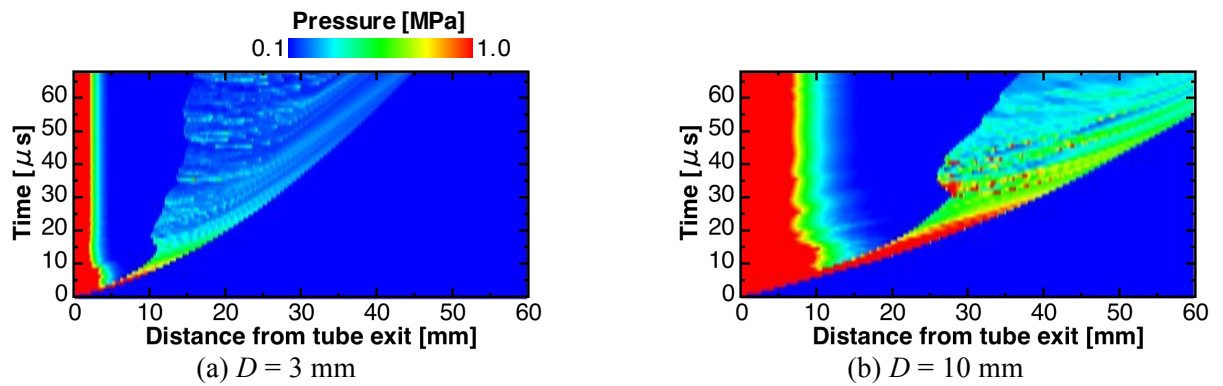


Figure 14. x - t diagram of pressure on the axis line outside the tube ($L = 90 \text{ mm}$, $P_{\text{H}_2} = 14.5 \text{ MPa}$)

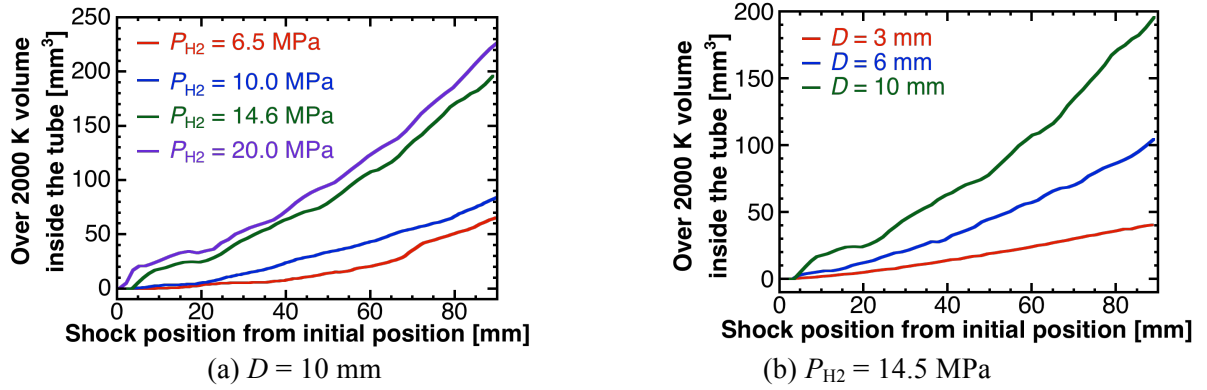


Figure 15. Over 2000 K volume inside the tube and shock position from initial position

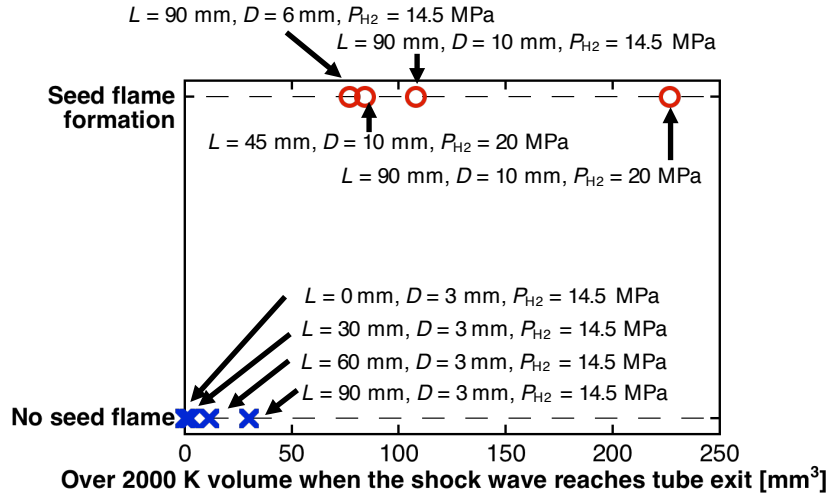


Figure 16. Over 2000 K volume when the shock wave reaches tube exit and seed flame formation

becomes longer by the three factors, namely, larger tube diameter, higher release pressure and longer tube length.

3.3 Seed flame formation and the ignited volume before the leakage

From the observation in the previous sections 3.1, the seed flame is formed by encompassing the ignited mixture in the recirculation zone near the tube edge. In addition, the larger amount of shock heated and the ignited volume raises the possibility of formation of the seed flame and develops larger seed flame. The tendency of the ignited volume by the tube diameter, tube length and release pressure is shown through the relationship between the over 2000 K volume inside the tube and the shock position from initial position in Fig. 15. Figure 15(a) shows the over 2000 K volume by different release pressure with $D = 10$ mm and Fig. 15(b) shows the over 2000 K volume for various tube diameter in the case of $P_{H_2} = 14.5$ MPa. Over 2000 K volume continues to increase as the shock wave propagates due to longer reaction and mixing time. Increasing release pressure makes the induction time short as Fig. 12 and reactivity improves, resulting in the larger over 2000 K volume in Fig. 15(a). Self-ignition of hydrogen occurs in contact surface near the axis line and the boundary layer whose surface area is proportional to the square of the tube diameter. Once the self-ignition occurs, larger tube diameter case has larger over 2000 K volume as shown in Fig. 15(b). Therefore, higher release pressure, longer tube length and larger tube diameter lead to larger ignited volume before the leakage from the tube. Figure 16 shows the relationship between the over 2000 K volume when the shock wave reaches tube exit and the formation of the seed flame. From Fig. 16, the seed flame is generated in the case that there is enough ignited volume to endure the heat loss and underexpansion at the time of leakage. The sufficient amount of the ignited volume is needed for the seed flame to be formed and sustained near the tube edge.

4.0 Conclusions

The two-dimensional axisymmetric numerical simulations with detailed reaction model are performed to clarify the effect of parameters on the behavior and duration of self-ignition of high pressure hydrogen released from the tube. The validation of the present numerical model is confirmed through the shock propagation speed and induction time of hydrogen-air mixture. Present numerical model shows good agreement with experimental and theoretical results for these two problems and can capture the compressible flow and chemical reaction correctly.

The strength of the spherical shock wave to keep chemical reaction and expansion are important factors for self ignited hydrogen jet to be sustained outside the tube. The trend of strength of spherical shock wave is enhanced by higher release pressure and larger tube diameter. The chemical reaction weakens due to expansion and the degree of expansion becomes larger as the spherical shock wave propagates. The characteristic time for the chemical reaction becomes shorter in higher release pressure, larger tube diameter and longer tube diameter cases from the induction time under constant volume assumption. The self ignited hydrogen jet released from the tube is sustained up to the distance where the characteristic time for chemical reaction is shorter than the characteristic time for the flow to expand, and higher release pressure, larger tube diameter and longer tube length expand the distance where the tip flame can propagate downstream.

For the formation of the seed flame which is the key for the jet fire, the velocity shear layer between the underexpanded hydrogen jet and ambient air generates the vortex from the edge of the tube and the ignited mixture is encompassed in the recirculation zone. The recirculation zone at the tube edge promotes the mixing and sustains the seed flame. The formation and stability of the seed flame depend on the amount of the ignited volume to overcome the heat loss and expansion. The larger amount of the ignited volume when the shock wave reaches the tube exit enhances the possibility of formation of the seed flame and develops larger seed flame. Longer tube length, higher release pressure and larger tube diameter lead to larger amount of the ignited volume.

References

1. Hans J. Pasman, William J. Roger, Safety challenges in view of the upcoming hydrogen economy : An overview, *Journal of Loss Prevention in the Process Industries*, **23**, 2010, pp. 697 – 704
2. Toshio Mogi, Yuji Wada, Yuji Ogata, A. Koichi Hayashi, Self-ignition and flame propagation of high-pressure hydrogen jet during sudden discharge from a pipe, *International Journal of Hydrogen Energy*, **34**, 2009, pp. 5810-5816
3. Toshio Mogi, Dongjoon Kim, Hiroumi Shiina, Sadashige Horiguchi, Self-ignition and explosion during discharge of high-pressure hydrogen, *Journal of Loss Prevention in the Process Industries*, **21**, 2008, pp. 199-204
4. Yeong Ryeon Kim, Hyoung Jin Lee, Seihwan Kim, In-Seuck Jeung, A flow visualization study on self-ignition of high pressure hydrogen gas released into a tube, *Proceedings of the Combustion Institute*, **34**, 2013, pp. 2057-2064
5. Qiangling Duan, Huahua Xiao, Wei Gao, Liang Gong, Jinhua Sun, Experimental investigation of spontaneous ignition and flame propagation at pressurized hydrogen release through tubes with varying cross-section, *Journal of Hazardous Materials*, **320**, 2016, pp. 18-26
6. J. X. Wen, B. P. Xu, V. H. Y. Tam, Numerical study on spontaneous ignition of pressurized hydrogen release through a length of tube, *Combustion and Flame*, **156**, 2009, pp. 2173-2189
7. M. V. Bragin, V. V. Molokov, Physics of spontaneous ignition of high-pressure hydrogen release and transition to jet fire, *International Journal of Hydrogen Energy*, **36**, 2011, pp. 2589-2596
8. Makoto Asahara, Akinori Yokoyama, A. Koichi Hayashi, Eisuke Yamada, Nobuyuki Tsuboi, Numerical simulation of auto-ignition induced by high-pressure hydrogen release with detailed reaction model: Fluid dynamic effect by diaphragm shape and boundary layer, *International Journal of Hydrogen Energy*, **39**, 2014, pp. 20378-20387

9. Hiroshi Terashima, Mitsuo Koshi, Chika Miwada, Toshio Mogi, Ritsu Dobashi, Effects of initial diaphragm shape on spontaneous ignition of high-pressure hydrogen in a two-dimensional duct, *International Journal of Hydrogen Energy*, **39**, 2014, pp. 6013-6023
10. Eisuke Yamada, Naoki Kitabayashi, A. Koichi Hayashi, Nobuyuki Tsuboi, Mechanism of high-pressure hydrogen auto-ignition when spouting into air, *International Journal of Hydrogen Energy*, **36**, 2011, pp. 2560-2566
11. M. V. Bragin, D. V. Makarov, V. V. Molkov, Pressure limit of hydrogen spontaneous ignition in a T-shaped channel, *International Journal of Hydrogen Energy*, **38**, 2013, pp. 8039-8052
12. H. C. Yee, Upwind and Symmetric Shock Capturing Schemes, NASA Technical Memorandum, 89464, 1987
13. Zekai Hong, David F. Davidson, Ronald K. Hanson, An improved H₂/O₂ mechanism based on recent shock tube/laser absorption measurements, *Combustion and Flame*, **158**, 2011, pp. 633-644
14. Hiroshi Terashima, Youhi Morii, Mitsuo Koshi, A ROBUST MULTI-TIME SCALE METHOD FOR STIFF COMBUSTION CHEMISTRY, *International Journal of Energetic Materials and Chemical Propulsion*, **14**, No. 3, 2015, pp. 177-196
15. Bonnie J. McBride, Sanford Gordon, Martin A. Reno, Coefficients for Calculating Thermodynamic and Transport Properties of Individual Species, NASA Technical Memorandum 4513, 1993
16. Sanford Gordon, Bonnie J. McBride, Frank J. Zeleznik, Computer Program for Calculation of Complex Chemical Equilibrium Compositions and Applications Supplement I – Transport Properties, NASA Technical Memorandum 86885, 1984
17. K. A. Bhaskaran, M. C. Gupta, TH. Just, Shock Tube Study of the Effect of Unsymmetric Dimethyl Hydrazine on the Ignition Characteristics of Hydrogen-Air Mixtures, *Combustion and Flame*, **21**, 1973, pp. 45-48
18. Chung K. Law, Combustion Physics, Cambridge University Press, 2006, pp. 14-50
19. V. P. Korobeinikov, Problems of Point-Blast Theory, American Institute of Physics, New York, 1991, pp. 65-116

Acknowledgments

This work is partially supported by “Joint Usage/Research Center for Interdisciplinary Large-scale Information Infrastructures” and “High Performance Computing Infrastructure” in Japan (Project ID : jh160020, hp160183). Part of the experimental results in this research were obtained using supercomputing resources at Cyberscience Center, Tohoku University.